

5-2013

## Enzyme Kinetics of Recombinant Human Arylsulfatase B (rhASB)

Katherine Marie Cunico  
*Dominican University of California*

<https://doi.org/10.33015/dominican.edu/2013.bio.02>

**Survey: Let us know how this paper benefits you.**

---

### Recommended Citation

Cunico, Katherine Marie, "Enzyme Kinetics of Recombinant Human Arylsulfatase B (rhASB)" (2013). *Graduate Master's Theses, Capstones, and Culminating Projects*. 61.  
<https://doi.org/10.33015/dominican.edu/2013.bio.02>

This Master's Thesis is brought to you for free and open access by the Student Scholarship at Dominican Scholar. It has been accepted for inclusion in Graduate Master's Theses, Capstones, and Culminating Projects by an authorized administrator of Dominican Scholar. For more information, please contact [michael.pujals@dominican.edu](mailto:michael.pujals@dominican.edu).

# **Enzyme Kinetics of Recombinant Human Arylsulfatase B (rhASB)**

A thesis submitted to the faculty of

Dominican University of California

&

BioMarin Pharmaceutical Inc.

in partial fulfillment of the requirements

for the degree

Master of Science

in

Biology

By

Katherine Cunico

San Rafael, California

May, 2013

**Copyright 2013 – by Katherine Cunico**  
**All Rights Reserved**

## CERTIFICATION OF APPROVAL

This thesis, written under the direction of the candidate's thesis advisor and approved by the Chair of the Master's program, has been presented to and accepted by the Faculty of Natural Sciences and Mathematics in partial fulfillment of the requirements for the degree of Master of Sciences in Biology at Dominican University of California and *BioMarin Pharmaceutical Inc.*.

Katherine Cunico, Candidate

Date 5/16/2013

Dr. Erno Pungor, Primary Thesis Advisor

Date 5/16/2013

Dr. Randall Hall, Secondary Thesis Advisor

Date 5/16/2013

Dr. Kiowa Bower, Chair

Date 5/16/2013

## Abstract

This project seeks to explain the enzyme kinetics of recombinant human Arylsulfate sulfatase B (rhASB) by using an *in vitro* bioassay and direct hydrolysis substrate assay to approach the problem of substrate limitation in establishing a representative  $k_{\text{cat}}$  for rhASB. The project also explores the makeup of a possible ASB complex within the cell. Previous published studies have sought to establish a turnover rate for rhASB, but have run into the problem of substrate limitation. Using a direct monosaccharide hydrolysis assay in conjunction with the same natural substrate bioassay, this project will attempt to provide insight to the  $k_{\text{cat}}$ , the turnover number, or number of reactions an enzyme can process,  $K_m$ , the substrate concentration at half enzyme saturation, and  $V_{\text{max}}$ , the maximum rate of the enzymatic reaction, for rhASB.

ASB deficient cells accumulate Chondroitin Sulfate and Dermatan Sulfate (CS/DS) products, the natural substrate of ASB. Incubating these cells and digesting the lysate with a CS/DS-specific lyase allows quantitation of CS/DS through fluorescent labeling and by capillary electrophoresis. In addition to a direct hydrolysis assay analyzed by High Pressure Liquid Chromatography (HPLC), this gives two potential methods of examining the kinetics of rhASB with both a monosaccharide substrate and the natural intracellular substrate

## **Table of Contents**

<b>List of Figures</b>	<b>6</b>
<b>List of tables</b>	<b>6</b>
<b>Introductions</b>	<b>7</b>
<b>Methods</b>	<b>14</b>
<b>Results and Discussion</b>	<b>17</b>
<b>Conclusion</b>	<b>30</b>
<b>References</b>	<b>31</b>

## List of Figures

Figure 2.1 N-acetyl-galactosamine With Possible Sulfation Sites	8
Figure 2.2 Capillary Electropherogram Showing Decrease of Residual Disaccharide Substrates	9
Figure 2.3 Dose Response Curve of Incubation of GM00519 Cells With rhASB	10
Figure 2.4 Estimation of the Apparent Average Catalytic Turnover Rate	11
Figure 2.5 Three Investigated Substrates of ASB	12
Figure 4.1.1 Depletion of Intracellular CS/DS by rhASB (passage 16)	17
Figure 4.1.2 Depletion of Intracellular CS/DS by rhASB (passage 14)	19
Figure 4.1.3 Average Turnover Rate for Cell Culture Assay	20
Figure 4.2.1 GalNAc-4S is Degraded by rhASB in the Hydrolysis Assay	21
Figure 4.2.2 Product Accumulation Rate As A Function of [GalNAc-4S] for 900pM rhASB	23
Figure 4.2.3 Hanes-Woolf Plot for the rhASB Hydrolysis Assay (900pM rhASB)	24
Figure 4.2.4 Investigation of Possible End-Product Inhibition of ASB	26
Figure 4.2.5 Hanes-Woolf Plots for 112pM Through 14pM rhASB	27
Figure 4.3.1 Silver Stain of BJ Fibroblasts	29

## List of Tables

Table 4.1.1 Incubation Concentrations and Internalized rhASB/well for Data Shown in Figure 4.1.1 and Figure 4.1.3	20
Table 4.2.1 Representative Data Set of the GalNAc-4S Hydrolysis Assay (900pM rhASB)	22
Table 4.2.2 Kinetics of the GalNAc-4S Desulfation with rhASB	25
Table 4.2.3 Average and Standard Deviations of $K_m$ and $k_{cat}$ values (900pM -14pM rhASB)	28

## Introduction

Enzyme kinetics studies the reaction rate at which enzymes process their substrates and is essential to understanding how diseases caused by enzyme malfunctions can be treated. Knowing an enzyme's reaction rate law provides insight into the mechanism of the reaction, whether or not the enzyme works in a complex, its role in the cell, how it is controlled, and from there, how a pharmaceutical product might inhibit, induce, or mimic the enzyme. Enzymatic mechanisms may depend on the amount and complexity of its substrates. When enzymes are involved in a complex mechanism, there is a rate determining step and that enzyme typically determines the overall reaction rate.

The two important parameters in enzyme kinetics are  $K_M$ , the substrate concentration at half saturation of the enzyme, and  $k_{cat}$ , the turnover rate. This represents the maximum number of possible enzymatic reactions per unit time. The relationship between these two parameters is described by the Michaelis-Menten equation for many enzyme reactions (W. Chen, 2010). Of course not all enzyme reactions fit this model, but establishing the relationship between the enzyme's turnover rate and relative substrate concentration is essential to understanding the kinetics of that enzyme.

Lysosomal storage diseases normally result when a single enzyme that is essential to the metabolism of lipids, glycoproteins, or mucopolysaccharides is absent or deficient. As lysosomes are responsible for the essential degradation of cellular nutrients, without the enzymes that metabolize them, partially degraded products accumulate in the cell and overcrowd the lysosome, resulting in enlarged and functionally disabled lysosomes and leading to disease phenotypes. As these diseases are caused by enzyme deficiencies or malfunctions, it is especially important to understand how the enzymes involved in normal processes function and at what rate so that normal function can be restored via proper enzyme replacement therapies (S. Bruni, 2007) (W-D Jin, 1992).

Mucopolysaccharidosis Type VI (MPS-VI, Maroteaux-Lamy Disease) is a lysosomal storage disease in which a deficiency in N-acetylgalactosamine-4-sulfate sulfatase (arylsulfatase B [ASB]) leads to an accumulation of the complex carbohydrates chondroitin sulfate (CS) and dermatan sulfate (DS) in the lysosomes (W-D Jin, 1992) (E.F. Neufeld, 1995). Severe phenotypes of MPS-VI include developmental and movement disorders due to this accumulation. ASB is a lysosomal exohydrolase that cleaves the sulfate groups at position 4 of the N-acetylgalactosamine (GalNAc) residues on the nonreducing ends of these glycosaminoglycan (GAG) structures. These GAGs are constitutively synthesized as part of the extracellular matrix and are essential components that are constantly recycled through endocytosis and transport into lysosome. This is a homeostatic process to ensure the quality of GAGs in the extracellular matrix. In lysosomal storage diseases the cycle is broken; in MPS-VI, these GAGs are not metabolized, leading to a chronic and progressive deterioration of the cells as partially degraded CS and DS build up within the lysosome.



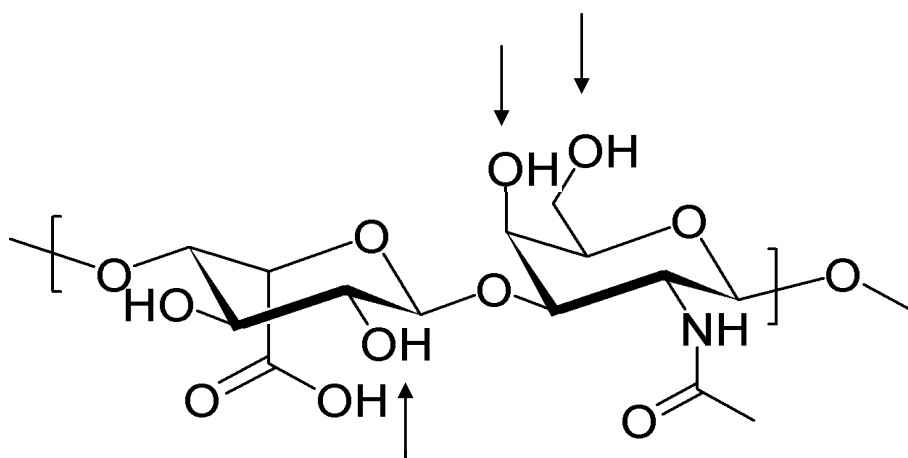


**Fig 2.1 N-acetyl-galactosamine with possible sulfation sites indicated by arrows.**

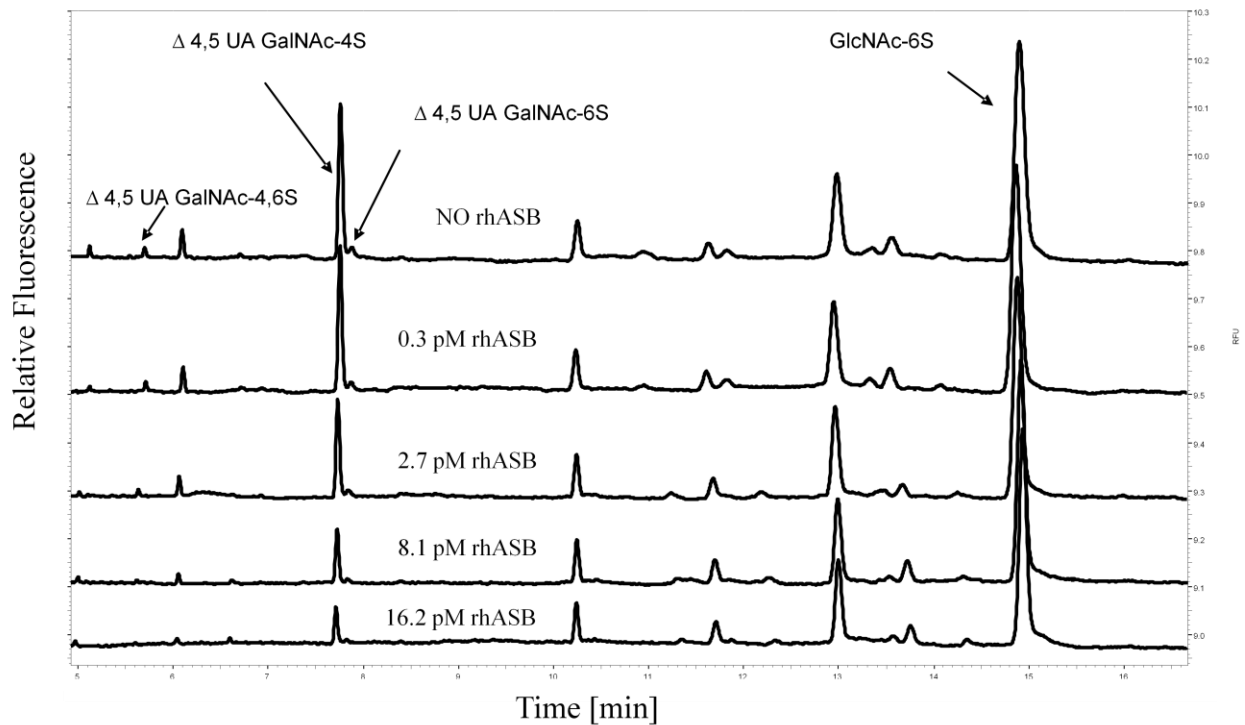
Chondroitin Sulfate and Dermatan Sulfate are the natural GAG substrates of ASB [Hopwood et al., 1986], and are made up of this GalNAc residue and an uronic acid component, either L-Glucuronic acid or L-Iduronic acid. The GalNAc residue can be sulfated on position 4, the most common form, and/or on position 6 (Kjellen and Lindahl, 1991). The enzyme rhASB enters target cells through the Cation Independent Mannose-6-Phosphate receptor (CI-MPR, also known as IGF2R) (Hille Rehfeld, 1995). ASB participates in the degradation of CS and DS as part of a multienzyme process involving, among others,  $\beta$ -hexosaminidase, iduronate-2-sulfatase and  $\alpha$ -iduronidase.

GM00519 cells isolated from an MPS VI patient are ASB deficient but possess the other lysosomal enzymes involved in the degradation of CS/DS. Therefore, the CS/DS that accumulates in the lysosomes of the GM00519 cells will only be partially hydrolyzed, with the degradation stopping when a GalNAc-4S residue is reached on the non-reducing end. This allows for GM00519 cells to be cultured and accumulate CS/DS within the cell culture without further cell growth, creating an ideal environment to study the kinetics of rhASB on its natural substrate when rhASB is supplemented in the culture medium. [Pungor et al, 2009].

Previous experiments have established colocalization of rhASB to the lysosome, as well as a basic dose response curve and turnover rate for the natural polysaccharide substrate, CS and DS (E. Pungor, 2009). CS/DS is measured as described below in Methods section. The studies have shown that ASB-deficient cells accumulate CS/DS in cultures post-confluence, consistent with the cells being able to synthesize CS/DS, secrete it, and then take them up into the lysosomes (Iozzo, 1998) (M. Fuller, 2004). The accumulated products were shown to be consistent with partial CS/DS degradation products from previous studies (W. Hoppe, 1988) (E. Pungor, 2009).

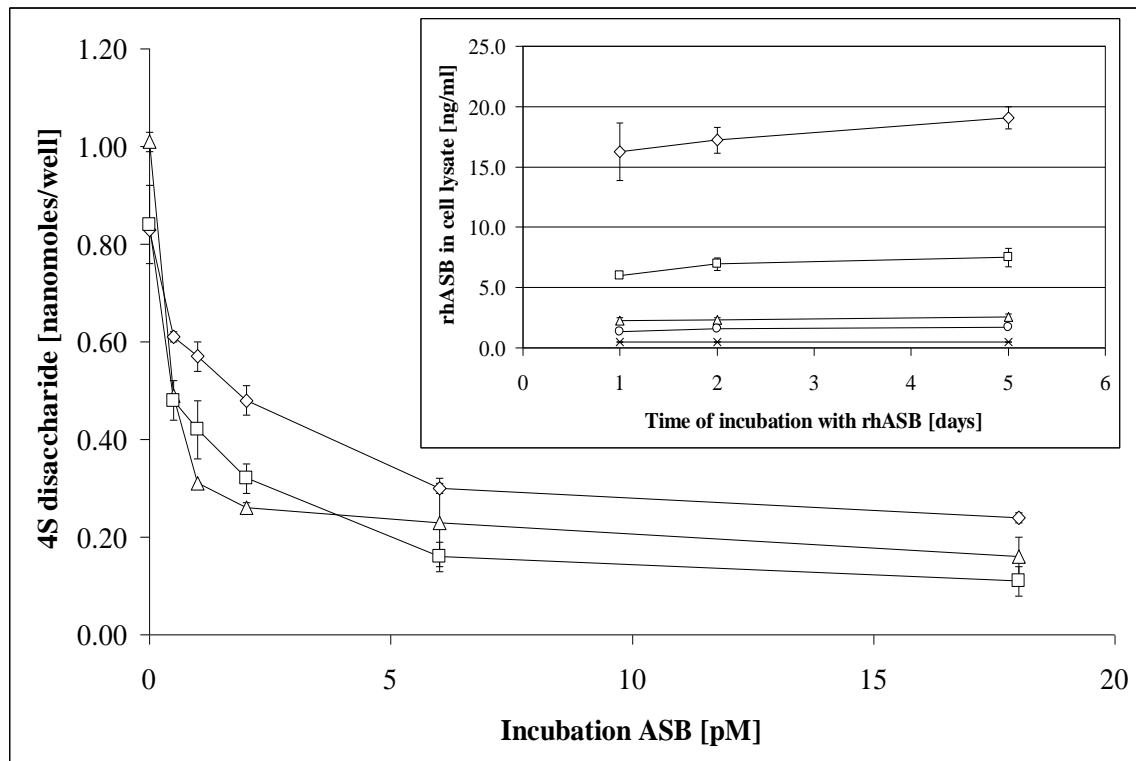
ASB was shown to be taken up and colocalized to the lysosome using confocal microscopy and fluorescent labeling secondary antibodies to detect LAMP1 (lysosome associated membrane glycoprotein 1) and ASB antibodies. (E. Pungor, 2009)

Figure 2.2 shows the degradation of the accumulated CS/DS in the GM00519 cells as a function of the increasing incubation concentration of rhASB. The accumulated GAGs can be visualized as peaks on the electropherogram and can be compared to the GlcNAc-6S internal standard peak for quantification. The dose-dependent response can be seen as the GalNAc-4S/6S peak decreases as the concentration of incubated ASB increases and the accumulated GAGs are degraded by the added ASB.



**Fig 2.2 Capillary Electropherogram showing the decrease in amount of all disaccharide substrates (4S-UA-GalNAc, 6S-UA-GalNAc, and 4,6S-UA-GalNAc) as the dose of rhASB with cells increases. (E. Pungor, 2009)**

Figure 2.3 shows similar data in a graphical curve, representing the dose-response curve of the accumulated GAGs to ASB. As more ASB is added to the system, more of the accumulated CS/DS is degraded. Eventually a plateau is reached as the enzyme concentration increases, consistent with levels of CS/DS present in lysates of healthy cells.



**Fig 2.3 A sample dose response curve** (outer graph) of 1-day (diamond), 2-day (triangle) and 5-day (square) incubation of rhASB. The inner graph shows the intracellular concentration of rhASB antigen in the cell lysate samples. (diamond: 18 pM; square: 6 pM; triangle: 2 pM; circle : 1 pM; X : no rhASB) (E. Pungor, 2009). These curves show a dose response with concentrations three orders of magnitude below the measured  $K_{\text{uptake}}$  from the cellular uptake assay.

From this degradation of CS/DS, an average turnover rate was calculated after extrapolating the amount of ASB present in each cell culture well as compared to the amount of GalNAc-4S degraded in each well. Figure 2.4 shows a representative graph of the calculated average turnover rate from this method.

Increasing the rhASB concentration or increasing the incubation time both led to decreased average reaction rates. However, an increase in incubation time and/or rhASB concentration still leads to decreased average turnover, indicating persistent substrate limitation. (E. Pungor, 2009)

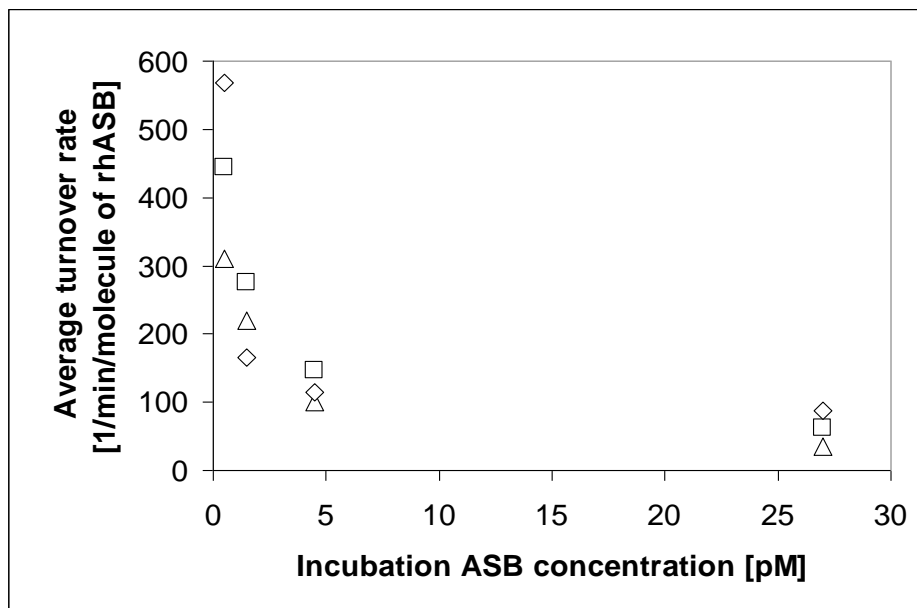


**Fig 2.4 An estimation of the apparent average catalytic turnover rate of the internalized rhASB was obtained.** (E. Pungor, 2009) Diamonds represent 1-day incubation; squares, 2 days; triangles, 5 days.

The enzymatic activity of rhASB can be tested in vitro using monosaccharide, oligosaccharide, or artificial substrates. The substrate widely used for ASB activity assays in published studies is a synthetic molecule, 4-methylumbelliferyl sulfate (4-MUS), which does not particularly resemble the in-vivo sulfate substrates. An investigation was performed at BioMarin to compare the functional performance of two different substrates, a labeled monosaccharide derived from dermatan sulfate: N-acetylgalactosamine-4-sulfate (4SGalNAc) and a trisaccharide substrate derived from dermatan sulfate: two 4SGalNAc moieties with an iduronic acid moiety in the middle.

Fig 2.5 shows the three investigated substrates for rhASB. The red circles indicate the sulfate moiety hydrolyzed by rhASB. Internal sulfates (such as the uncircled sulfate shown in the trisaccharide structure above) are not hydrolysable by ASB.

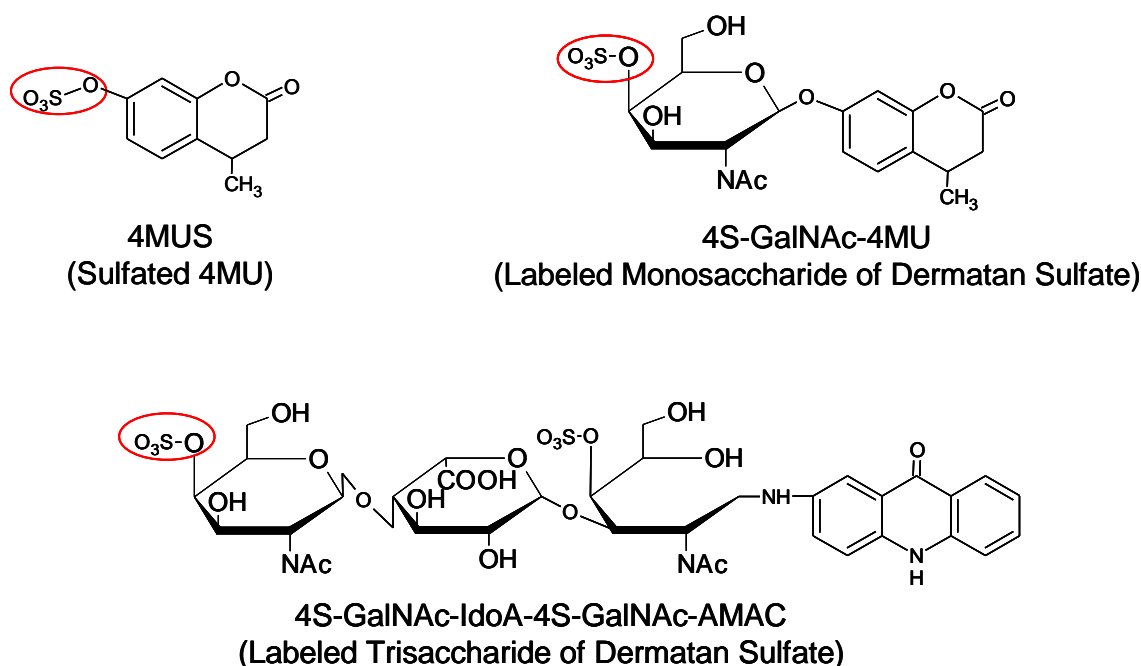


**Figure 2.5 Three investigated substrates of ASB**

4-MUS, the synthetic substrate, has a  $k_{\text{cat}}$  of about 14,400 molecules per minute, while the more natural substrates have a  $k_{\text{cat}}$  ranging down to 18 molecules/min for the monosaccharide substrate, and 7 molecules/minute for the trisaccharide. However,  $K_M$  values for the more natural substrates suggest tighter binding than the 4-MUS substrate, with values in the  $\mu\text{M}$  range for the trisaccharide substrate, over two orders of magnitude higher than either the 4-MUS or the monosaccharide substrate.

As rhASB is only capable of cleaving the 4-sulfate from GalNAc only on the reducing end, if it alone acted on a GAG oligosaccharide, it could not hydrolyze the nonterminal GalNAc. Previous analysis showed that the predominant fractions in CE analysis would have had to be derived from intrachain resides in the CS/DS chains. (E. Pungor, 2009) This means that rhASB needs to cooperate with other lysosomal enzymes involved in the degradation, possibly through the formation of a lysosomal degradation complex to process GAG oligosaccharides.

There are three specific aims of this thesis. The first is to establish enzyme kinetics of rhASB when supplied to ASB-deficient cells. By culturing ASB-deficient cells and accumulating CS/DS within these cells and then incubating them with various concentrations of ASB, the turnover rate of rhASB can be observed and measured if ASB is the rate limiting factor by determining the rate of CS/DS degradation and the intracellular (intra-lysosomal) concentration of the supplied ASB.

The second aim is to examine and establish a  $K_M$  and  $k_{\text{cat}}$  for rhASB with the monosaccharide substrate GalNAc-4S. From previous experiments, a much slower turnover rate was observed in

an activity assay as opposed to the previous artificial substrate, 4-methylumbelliferyl sulfate, and an even slower turnover rate was observed with a trisaccharide structure resembling a longer GAG chain. By developing a direct hydrolysis assay to measure the degradation of GalNAc-4S by rhASB, a  $k_{\text{cat}}$ ,  $K_M$ , and  $V_{\text{max}}$  can be established

The third aim is to isolate and define the complex we theorize ASB to work with in the lysosome. As ASB can only clip its substrates in specific locations it is possible that it forms a complex with other enzymes involved in degrading CS and DS in the lysosome. By culturing both ASB deficient and fully competent cells, lysing them, and running them through a Size-Exchange Chromatography (SEC) column, where single molecules of ASB should run can be determined. Peaks with ASB activity that are of larger molecular weight, implying a complex formation can then be isolated and characterized.

### 3. METHODS

#### 3.1 Intracellular activity of rhASB in GM00519 cells

##### 3.1.1 Cell culture

GM00519 fibroblast cells, isolated from an MPS VI patient [Jin et al., 1992], were obtained from Coriell Institute for Medical Research. Cells were cultured on 12 well plates in DMEM (Irvine Scientific) supplemented with 4.5 g/L glucose, 10% FBS and 2mM L-Glutamine (37°C and 5% CO<sub>2</sub>). Cells were plated at approximately 50% confluence. Typically the cultures reached confluence within 4-7 days after plating. Cultures were maintained for 4-5 weeks post confluence. Medium was replaced every 3-5 days.

BJ normal foreskin fibroblasts (ATCC) were cultured on 12 well plates in MEM (ATCC) supplemented with 10% FBS for 3-6 weeks post confluence. Medium was replaced every 2-3 days.

Cells were harvested, washed twice in PBS and lysed in M-PER Mammalian Protein Extraction Reagent (Pierce), the lysates were centrifuged at 14000g for 10 minutes and supernatants were collected.

##### 3.1.2 Enzyme uptake

For enzyme uptake, rhASB (from BioMarin Pharmaceutical Inc.) was added to the culture medium of the GM00519 cells at various concentrations and for various periods of time (1 to 5 days) for the last part of the cell culture. Medium was replaced every 3-5 days.

##### 3.1.3 Analytical methods

###### 3.1.3.1 ASB in cell lysates

The concentration of rhASB in the cell lysate was measured by an ELISA. Polyclonal antibodies were generated by immunizing rabbits and a sheep with a highly purified preparation of rhASB followed by purification of total IgG fraction from antisera (Rab-anti-rhASB IgG and Sheep-anti-rhASB IgG) using Protein G affinity chromatography. Rabbit anti-rhASB IgG was also conjugated to horseradish peroxidase (HRP) to generate the detecting antibody HRP-Rab anti-rhASB IgG. A Nunc MaxiSorp immunoplate was coated with Rabbit anti-rhASB IgG at 2 µg/mL in carbonate buffer (pH 9.5) for 2 hr at 37°C. The plate was washed with 1X D-PBS (Mediatech) containing 0.1% polysorbate-20 and then blocked with D-PBS containing 2% BSA and 0.05% polysorbate-20 for 1 hr at 37°C. Samples and rhASB reference standard were diluted in the blocking solution and applied to wells, and incubated for 1 hr at 37°C. After washing, the wells were incubated for 30 min at 37°C with HRP-Rabbit anti-rhASB IgG diluted in blocking solution. After washing, the TMB substrate reagent (Bio-Rad Laboratories) was added to the

wells and incubated for 15 min at 37°C, followed by adding 2N H<sub>2</sub>SO<sub>4</sub> stop solution. Absorption at 450 nm was read in a microplate spectrophotometer (Molecular Devices).

Total protein concentrations of cell lysates were determined by the BCA method (Pierce) in relation to a BSA standard curve.

#### 3.1.3.2 DS/CS in cell lysates

Chondroitin ABC lyase (EC 4.2.2.4., BioMarin Pharmaceutical Inc.) was dissolved in 50 mM TRIS, pH 8.2 at 2.5 mg/mL. 10 µL of this solution was added to the centrifuged cell lysate supernatant (50 µL) for overnight digestion at 37 °C.

The digest was then dried in a centrifugal vacuum evaporator. N-acetylglucosamine-6-sulfate GlcNAc-6S (Sigma) was added as internal standard (20 µL of 0.05 mM GlcNAc-6S in water, 1 nMole) to the sample and the sample was dried again in a centrifugal vacuum evaporator.

The digestion products were labeled by first adding 6µL of 15% acetic acid to the dried sample followed by adding 3 µL of the 2-amino-acridone reagent (AMAC, Invitrogen, 15 µg/µL in DMSO) and 10 µL of Na-cyanoborohydride. The mixture was incubated for 24 hours at 37 °C. After incubation, the sample was reconstituted in 50 µL of water and centrifuged at 14,000g for at least 5 minutes.

The labeled disaccharides in the sample were analyzed by Capillary Zone Electrophoresis (CZE) using a Beckman PA800 system equipped with a Laser Induced Fluorescence (LIF) detector (Beckman Coulter). NCHO capillary and the NCHO buffer kit (Beckman Coulter) were used for the separation. The samples were injected by pressure (0.5 p.s.i., 10 s) into the capillary, and the separation was performed at 18 kV (0.18 minute ramp, reverse polarity).

Identification of the DS/CS digestion peaks was previously performed using the disaccharide standards: L-Δ<sup>4</sup>,5-UA-β(1-3)-D-GalNAc (0S disaccharide), L-Δ<sup>4</sup>,5-UA β(1-3)-D-GalNAc-4S (4S disaccharide), L-UA β(1-3) -D-GalNAc β-6S (6S disaccharide), L-UA β(1-3)-D-GalNAc β-4,6S (4,6S disaccharide) and L-UA-2S β(1-3)-D-GalNAc β (2S disaccharide) (all from Oxford Glycosystems).

#### 3.2 Activity of the rhASB on N-acetylgalactosamine-4-sulfate (GalNAc-4S)

N-acetyl-D-galactosamine-4-O-sulphate (Carbosynth; 10mg in 1mL water to 3.2mM) was diluted to 800uM in 10mM NaOAc pH 5.0 as an assay buffer, then further diluted in two-fold series down to 12.5uM. 40uL of these substrate dilutions were mixed with 10uL rhASB at concentrations ranging from 3.58nM to 7pM and incubated for 2 hours at 37C. The reaction was stopped by heating for 15 minutes in a 95C heat block.

The samples were analyzed by HPLC using a Dionex ICS-5000 system, a CarboPac PA1 4x250mm carbohydrate column for the separation and Pulsed Electrochemical Detection. The



samples were injected at 1.0mL/min into a multi-step gradient of water (A), 200 mM NaOH (B), and 200mM NaOH + 500mM NaOAc (C) (start at 46% B, 14% C, ramp to 0% B 60% C at 10 min, ramp to 100% C at 17 min, and ramp down to 46% B and 14%C at 19.5 min) for a total analysis time of 26 minutes.

### 3.3 Attempts to Isolate an Intracellular ASB Complex

#### 3.3.1 Cell Culture

GM00519 and BJ fibroblasts were grown as above and cultured for 3-5 weeks past confluence. GM00519 cells were incubated with 0, 1nM, 100pM, and 10pM ASB for 5 days, then lysed with IP Lysis Buffer (Thermo). Lysates were centrifuged at 14,000g for 10 minutes and supernatants were collected.

#### 3.3.2 HPLC

Samples were run on an Agilent 1200 series HPLC system, using a TOSOH G4000SWx1 7.8x30mm column. 100uL of sample was injected at 0.5ml/min for 30 min, using 60mM NaOAc pH 5.6 as mobile phase.

Fractions were collected in minute intervals.

#### 3.3.3 ASB Activity Assay

Prepared 4-MUS substrate (1mM, BioMarin) was placed in a water bath at 37°C. 50µL of collected HPLC fractions per well was added to a 96-well plate, with a set of duplicates for each. A standard curve with dilutions of 4-MU ranging from 100uM – 5uM was also prepared. Each concentration of 4-MU was dispensed in duplicate, 50µL per well. The plate was incubated at 37°C for 20 minutes in an incubator. At the end of the incubation, 100uL per well of pre-warmed 4-MUS was added to the samples. The plate was incubated for another 20 minutes at 37°C in an incubator. The reaction was stopped by adding 150 µL per well of glycine/carbonate stop buffer (pH 10.5). The fluorescence of the plate was read with an excitation of 366 and an emission of 466 using a SpectraMax Gemini fluorescent plate reader. SOFTmax Pro Data software was used to calculate standard curves and backcalculate sample ASB concentrations.

## 4. Results and Discussion

### 4.1 Intracellular Activity of rhASB in GM00519 Cells

rhASB deficient GM00519 cells, when plated and grown post-confluence for 3-5 weeks, accumulate CS and DS in the lysosome at levels detectable by lysing the incubated cells, digesting the CS/DS with Chondroitin ABC lyase to digest the polysaccharide chain into defined building block disaccharides, labeling these resulting disaccharides with a neutral dye, and detecting them by capillary zone electrophoresis (CZE). By adding an internal standard, the residual CS/DS after incubation of the cells with rhASB when supplemented into the media can be quantified. As the cells take up the ASB within the media, the rhASB degrades the accumulated CS/DS in a dose-dependent manner and the degradation of CS/DS can be quantified and a relative degradation rate can be calculated.

The data presented below are representative subsets of the data generated over months of optimization of assay conditions

Figure 4.1.1 shows the residual CS/DS in the GM00519 cells after supplementation of rhASB into the culture medium for five days (GM00519 cells were cultured for five weeks post-confluence before incubation with rhASB). In agreement with published experiments, a non-zero plateau is reached at higher incubation concentrations of rhASB. This level is equivalent to the level of CS/DS present in non-rhASB-deficient BJ fibroblasts (data not shown).

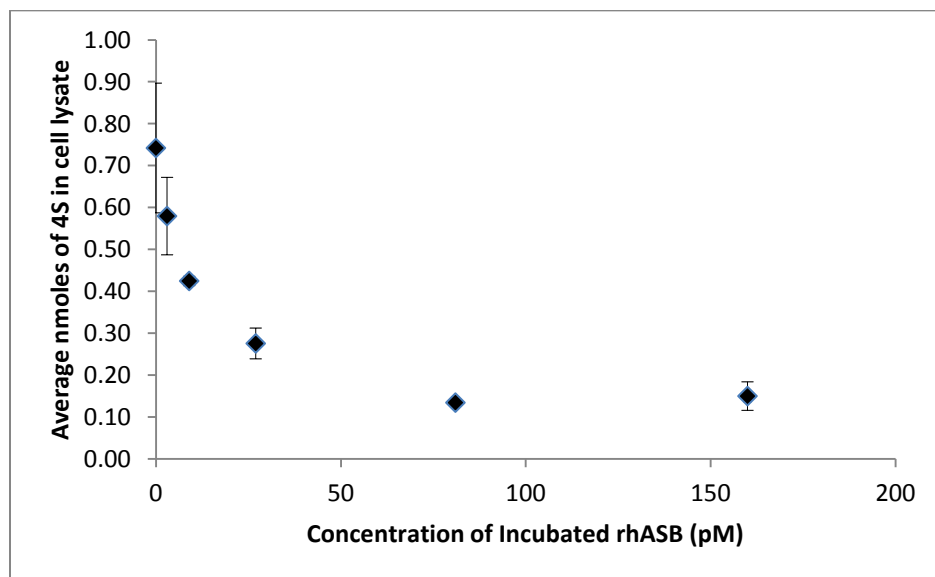


**Figure 4.1.1 Depletion of intracellular CS/DS by incubating GM00519 cells with rhASB (passage 16)** The error bars represent the standard deviation (2 wells) for each incubation concentration. GM00519 cells were incubated with 0, 3, 9, 27, 81, and 162 pM of rhASB for five days.

While the amount of accumulated CS/DS digested by the added rhASB is dependent on the dose of rhASB added to the media, there is no appreciable linear response, as seen in Figure 4.1.1. Assuming that the intracellular concentration of the enzyme is proportional to the incubation concentration (Pungor, 2009), this is an indication of substrate limitation in the assay. In order to overcome this substrate limitation, two approaches were taken. First, we attempted to find conditions where the CS/DS accumulation is higher in the GM00519 cells in an attempt to increase the starting substrate concentration. Second, we attempted to decrease the rhASB incubation concentration and improve the sensitivity of the ELISA to be able to detect lower concentration of ASB in the lysates so as to be able decrease the incubation concentration of enzyme in the assay.

Experiments were performed with earlier passage number cultures, and upon analysis, it became transparent that these “younger” GM00519 cells accumulate CS/DS faster. Unfortunately, however, these cultures also had a dramatically reduced dynamic range in the assay; the steady state levels of residual CS/DS at high ASB incubation concentrations were much higher than with higher passage numbers.

The observed depletion of CS/DS in Figure 4.1.3 is consistent with previous observations (Pungor 2009), where the difference of one passage age of cells resulted in a two-fold difference in CS/DS intracellular accumulation. The high residual, non-depletable CS/DS is most likely a result of the higher CS/DS production rate. Experiments performed with lower passage number cultures (e.g. passage 11 and passage 12) also exhibit this high CS/DS accumulation rate and high residual CS/DS level (data not shown).

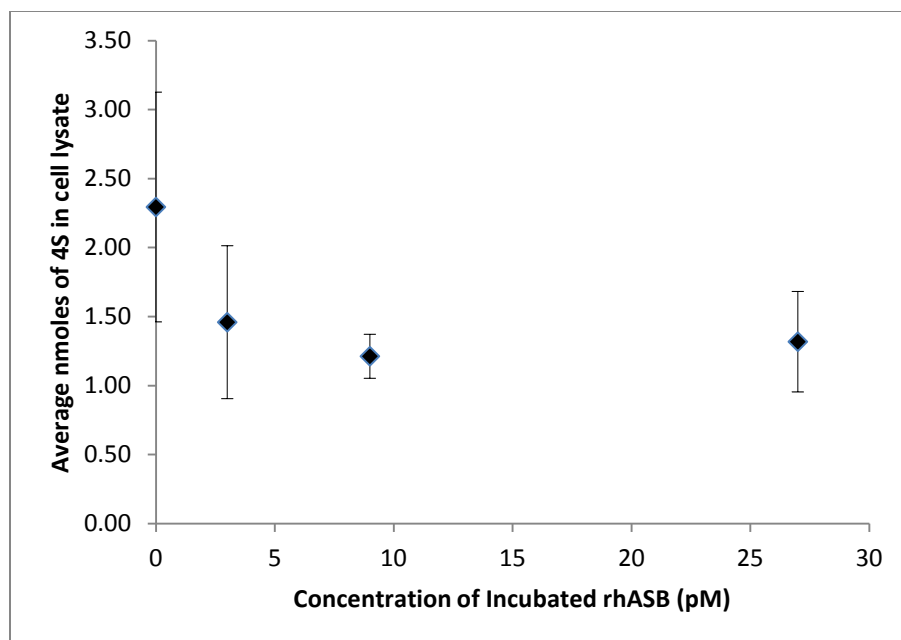


**Figure 4.1.3 Depletion of intracellular CS/DS by incubating GM00519**

**cells with rhASB (passage 14)** The error bars represent the standard deviation (3 wells) for each incubation concentration. GM00519 cells were incubated with 0, 3, 9, and 27 pM of rhASB for five days.

Lysates from GM00519 cells incubated with rhASB were also tested in an ELISA to determine the amount of rhASB present in the cell so that turnover rates for the assay can be calculated. As the incubation concentration of rhASB was in the pM range, the sensitivity of the ELISA had to be investigated and optimized. Unfortunately, increasing the sensitivity also raised the background noise of the assay, limiting the data points that could be used. Due to the high background of the ELISA, data points from ASB incubation concentrations below 27pM were excluded. To offset this, more dilutions were performed in the lowest concentration region to generate more independent measurements on turnover rates.

Turnover rates were calculated as average turnover rates for the incubation time with the rhASB using the molar CS/DS depletions and the intracellular ASB concentrations statistically different from the baseline. GM00519 cell lysates that had not been incubated with rhASB were to determine the initial accumulated CS/DS concentrations for GM00519 cells.

Figure 4.1.4 shows the calculated turnover rates for the 5 day incubation experiment shows in Figure 4.1.1 (passage 16) and Table 4.1.1 shows the amounts of internalized ASB by the cells in the assay well for these points.

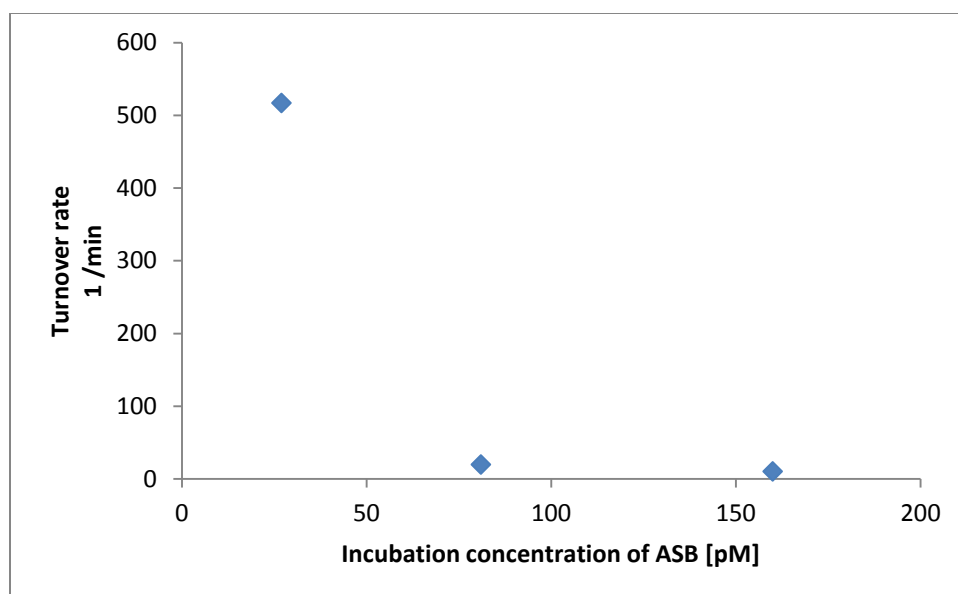


**Figure 4.1.4 Average Turnover Rate for Cell Culture Assay (Passage 16)**

Incubation Concentration ASB	Internalized ASB/well	Turnover Rate (1/min)
27 pM	0.13 pmol	517
81pM	4.24 pmol	20
160 pM	7.9 pmol	10

**Table 4.1.1 Incubation Concentrations and Internalized ASB/well for data shown in Figure 4.1.1 and Figure 4.1.4.**

Using data from the publication, the 1, 2, and 5 day incubation experiments (Figure 4, Pungor 2009) at a 27pM ASB incubation concentration resulted in average turnover rates of 87.3, 1 day; 62.1, 2 day; and 35.1, 5 day.

Although there are significant differences between these two sets of data (most likely caused by the noise from altering the sensitivity of the ELISA), these new experiments confirm that the turnover rate measured with the polysaccharide chain, degraded in the lysosome by an enzyme system in which the rate was controlled by the ASB supplied, can be significantly higher than the turnover rates observed with short-chain oligosaccharide substrates of rhASB in an optimized direct assay (as discussed in Introduction). This supports the hypothesis that CS/DS is degraded by a different mechanism within the lysosome, supporting the hypothesis of the existence of a GAG-degrading complex within the lysosome of which ASB is a part.

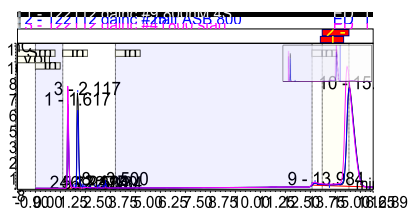
## 4.2 Activity of rhASB on N-acetylgalactosamine-4-sulfate (GalNAc-4S)

In this direct hydrolysis assay, the monosaccharide substrate GalNAc-4S and rhASB are incubated together for a predetermined length of time (in the experiments below the exposure times were two hours [one hour where noted]). Analysis by Strong Anion Exchange (SAE) HPLC with pulsed electrochemical detection allows for the measurement of the substrate GalNAc-4S and the end product GalNAc.

The data shown below represents several experiments performed to adjust and optimize the assay.

The dilution range of 800 $\mu$ M-12.5 $\mu$ M for GalNAc-4S and a starting incubation of 3.58nM rhASB were decided upon after determining the detection limits of the SAE HPLC.

Figure 4.2.1 shows that during incubation with rhASB, GalNAc is produced as a result of degradation of the GalNAc-4S sample by ASB. There is no GalNAc peak in the chromatogram of the GalNAc-4S standard (pink trace), but after incubation with ASB, regardless of the concentration supplied, the concentration of GalNAc increases drastically (blue and black traces). The GalNAc-4S standard sample also has the highest concentration of GalNAc-4S present, showing that GalNAc-4S is degraded by the inclusion of rhASB.



GalNAc

GalNAc-4S

**Figure 4.2.1 GalNAc-4S is degraded by ASB in the hydrolysis assay**

The peak at 2.117 minutes is GalNAc and the peak at 15.7 is GalNAc-4S. The pink trace represents the

800  $\mu$ M GalNAc 4S sample before incubation with ASB; blue, the 800 $\mu$ M GalNAc sample incubated with 1.8nM ASB; black, the 800 $\mu$ M GalNAc sample incubated with 3.58nM ASB.

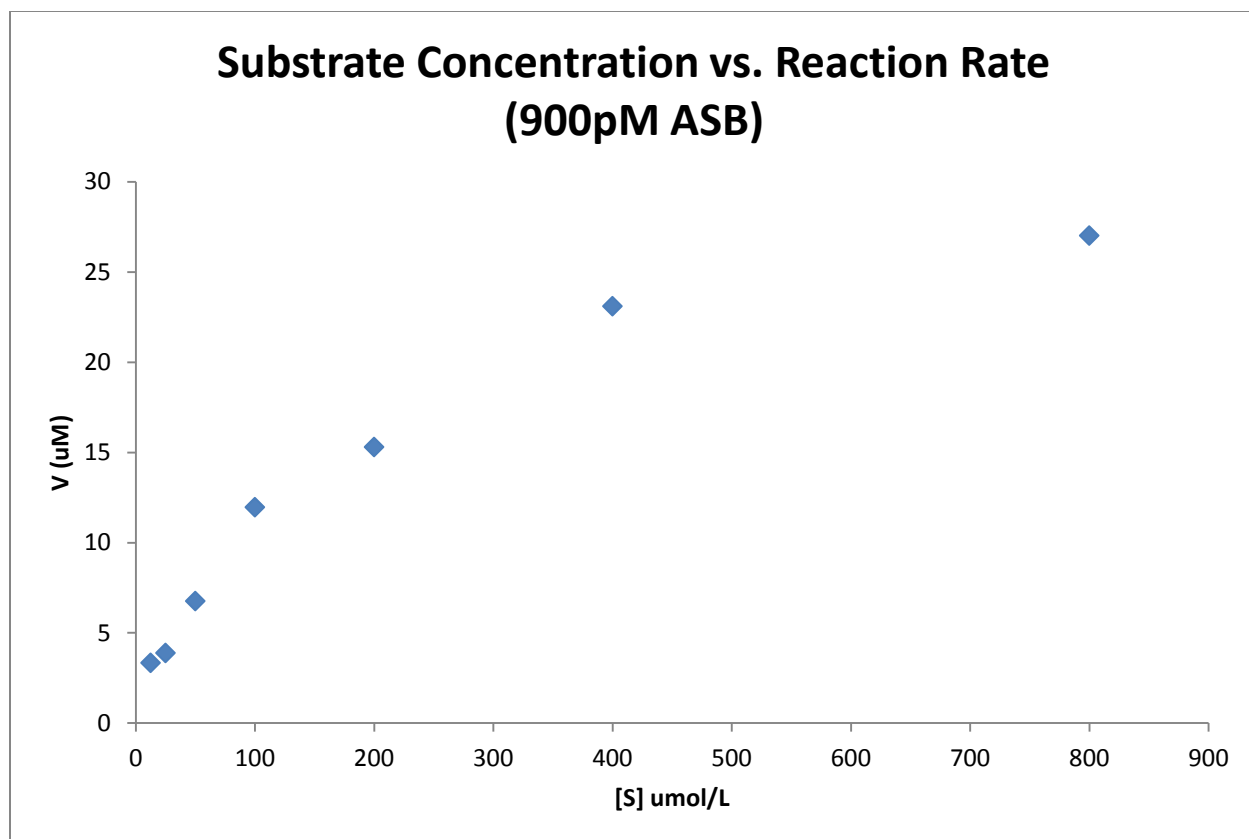
The peak at 1.617 is most likely the heat-denatured rhASB from boiling the reaction mixture to stop the enzymatic reaction and is present in comparable amounts in all reactions.

Table 4.2.1 shows a representative data set generated by the GalNAc-4S hydrolysis assay (900pM rhASB with a dilution series of GalNAc-4S ranging from 800 $\mu$ M to 12.5 $\mu$ M). The concentration of GalNAc produced is back-calculated with the use of a GalNAc standard curve. This concentration represents the reaction rate  $v$  and is used to show the product accumulation rate as a function of the initial substrate concentration [S].

**Table 4.2.1 Representative Data Set of the GalNAc-4S Hydrolysis Assay (900pM ASB)**

Supplied [GalNAc-4S] ([S])( $\mu$ M)	GalNAc product (peak area)	[S] ( $\mu$ M)	GalNAc ( $\mu$ M)	Rate of GalNAc Accumulation ( $v$ ) ( $\mu$ M/min)	[S]/ $v$ (min)
800	27	800	56.7	0.49	1636
400	23.1	400	50	0.42	959.2
200	15.3	200	32.8	0.27	731.1
100	12	100	25.5	0.21	471.1
50	6.8	50	14	0.12	428.7
25	3.4	25	7.6	0.06	392.2
12.5	3.3	12.5	6.4	0.05	232.8

Figures 4.2.2 and 4.2.3 shows plots of the data in Table 4.2.1. As shown in Figure 4.2.2, the reaction rate and the initial substrate concentration show a hyperbolic relationship.



**Figure 4.2.2 Product accumulation rate as a function of [GalNAc-4S] for 900pM rhASB**

Michaelis-Menten enzyme kinetics provides a mechanistic explanation for the hyperboloid response observed for enzymatic reactions,

$$v = \frac{d[P]}{dt} = V_{\max} \frac{[S]}{K_m + [S]} = k_{\text{cat}}[E]_0 \frac{[S]}{K_m + [S]}$$

where  $v$  is the reaction rate (product accumulation rate),  $V_{\max}$  is the maximum reaction rate achieved,  $K_m$  is the substrate concentration ( $[S]$ ) at which the reaction rate is half of  $V_{\max}$ ,  $[E]_0$  is the enzyme concentration, and  $k_{\text{cat}}$  is the turnover rate.

The different rate constants of the Michaelis-Menten equation can be easily calculated by performing a linear transformation of the original equation.

In order to linearize the Michaelis-Menten equation, several approaches can be used. Figure 4.2.3 shows the Hanes-Woolf plot using the rearrangement of the Michaelis-Menten equation,

$$\frac{[S]}{v} = \frac{1}{V_{\max}}[S] + \frac{K_m}{V_{\max}}.$$

The slope of the  $[S]/v$  vs.  $[S]$  plot is  $1/V_{\max}$ , and the intercept is  $K_m/V_{\max}$ . The Hanes-Woolf plot of the data in Table 4.2.1 is shown in Figure 4.2.3.



A representative turnover rate can be calculated by arranging the Michaelis-Menten equations further to give

$$V_{\max} = k_{\text{cat}}[E]_0.$$

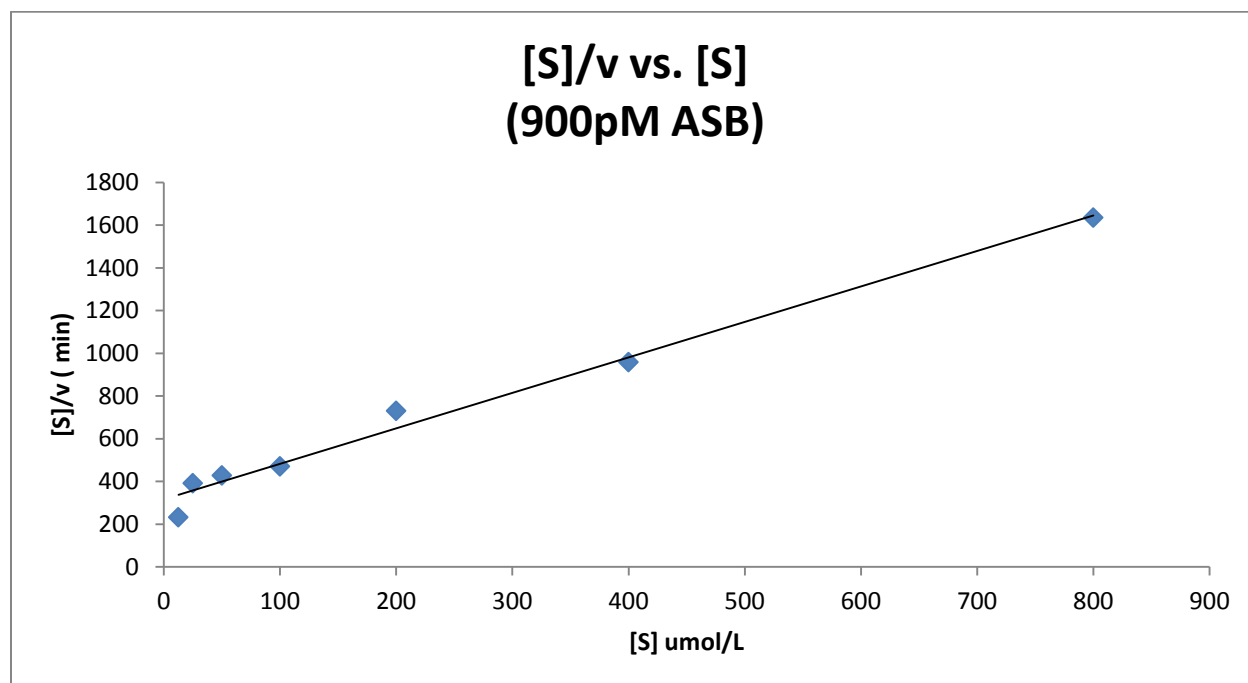


**Figure 4.2.3 Hanes-Woolf plot for the ASB hydrolysis assay (AS B concentration: 900pM)** The linear regression has a correlation coefficient of 0.993.

The linear regression from the data plotted in Figure 4.2.3 has a calculated  $K_m$  of 190.2 and apparent  $k_{\text{cat}}$  of 668.6 1/min.

Several reactions were performed with decreasing concentrations of incubated rhASB in an attempt to further explore the hydrolysis kinetics of GalNAc-4S and rhASB.

**Table 4.2.2 Kinetics of the GalNAc-4S desulfation with rhASB**

<b>Concentration of ASB</b>	<b>Reaction time (hour)</b>	<b>K<sub>m</sub> (uM)</b>	<b>k<sub>cat</sub> (1 /min)</b>
<b>35.8 nM</b>	2	67.1	79
<b>3.58 nM</b>	2	178.4	305.1
<b>1.8 nM</b>	2	143.5	533.1
<b>900 pM</b>	2	190.2	668.6
<b>450 pM</b>	2	202.2	1012.4
<b>112 pM</b>	1	390.9	820.9
<b>56 pM</b>	1	112.2	1053.6
<b>28 pM</b>	1	96.9	686.1
<b>14 pM</b>	1	107.2	692.2

As shown in Table 4.2.2, decreasing the rhASB concentration from 35.8 nM to 450 pM resulted in increasing calculated k<sub>cat</sub> values ( from 79 to 1655 1/min) and a lesser increase in the calculated K<sub>m</sub>. This indicates that the reaction does not closely follow Michaelis-Menten kinetics under these conditions; if it did follow the Michaelis-Menten model, both parameters should be constant.

One possible explanation for this observation could be an end-product inhibition. Sulfate is a known millimolar inhibitor of ASB (Hopwood, 1986). In an attempt to remove free sulfate generated by the enzyme from the reaction mixture, the hydrolysis assay was performed in the presence of 50mM BaCl<sub>2</sub>. The solubility product of BaSO<sub>4</sub> is  $1.08 \times 10^{-10}$ . Adding in 50mM of BaCl<sub>2</sub> supplies the reaction with enough free barium ions to keep the concentration of free sulfate groups within the reaction below 50nM. If more sulfate than that were present, the free barium ions would bind and precipitate as BaSO<sub>4</sub>.

Figure 4.2.4 shows that the presence of 50mM BaCl<sub>2</sub> did not change the apparent kinetics of the hydrolysis; the apparent k<sub>cat</sub>s were comparable (266.885 molecules/min for the reaction run without BaCl<sub>2</sub>, and 252.354 molecules/min for the reaction run in the presence of BaCl<sub>2</sub>).

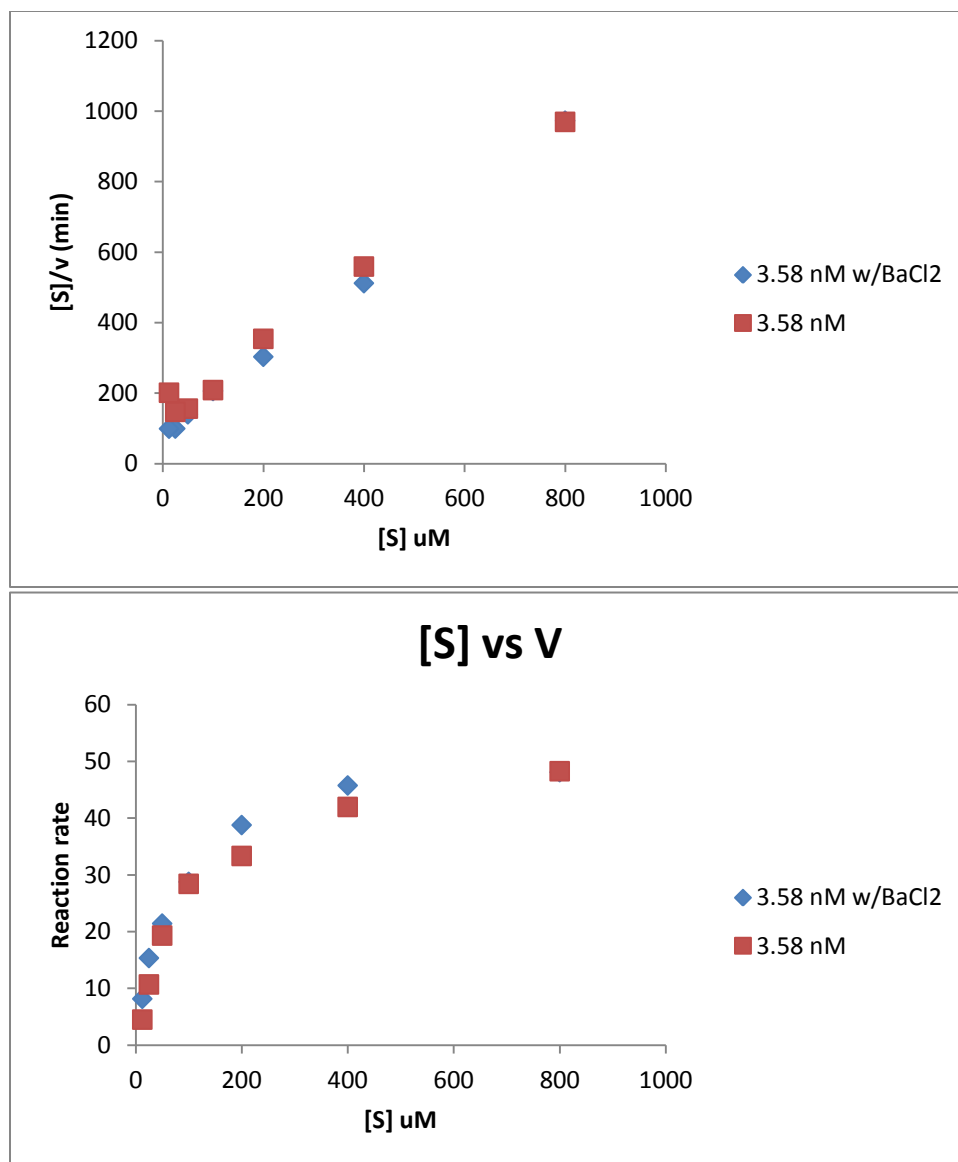


**Figure 4.2.4 Investigation of possible end-product inhibition of ASB through the use of BaCl<sub>2</sub>**

While adding BaCl<sub>2</sub> to the system was unsuccessful at altering the observed enzyme kinetics, it is possible the free sulfate groups produced bind to the active site of rhASB, where they are inaccessible to bind to the free barium ions, but can still block the activity of rhASB. Decreasing the reaction time to an hour was an attempt to minimize this possible end-product inhibition.

Working with very small concentrations of ASB and thus very small resulting concentrations of the GalNAc product led to high noise in the chromatography assay, but even under these conditions, a strong linear correlation can still be seen in the resulting Hanes-Woolf plots, shown below in Figure 4.2.5.

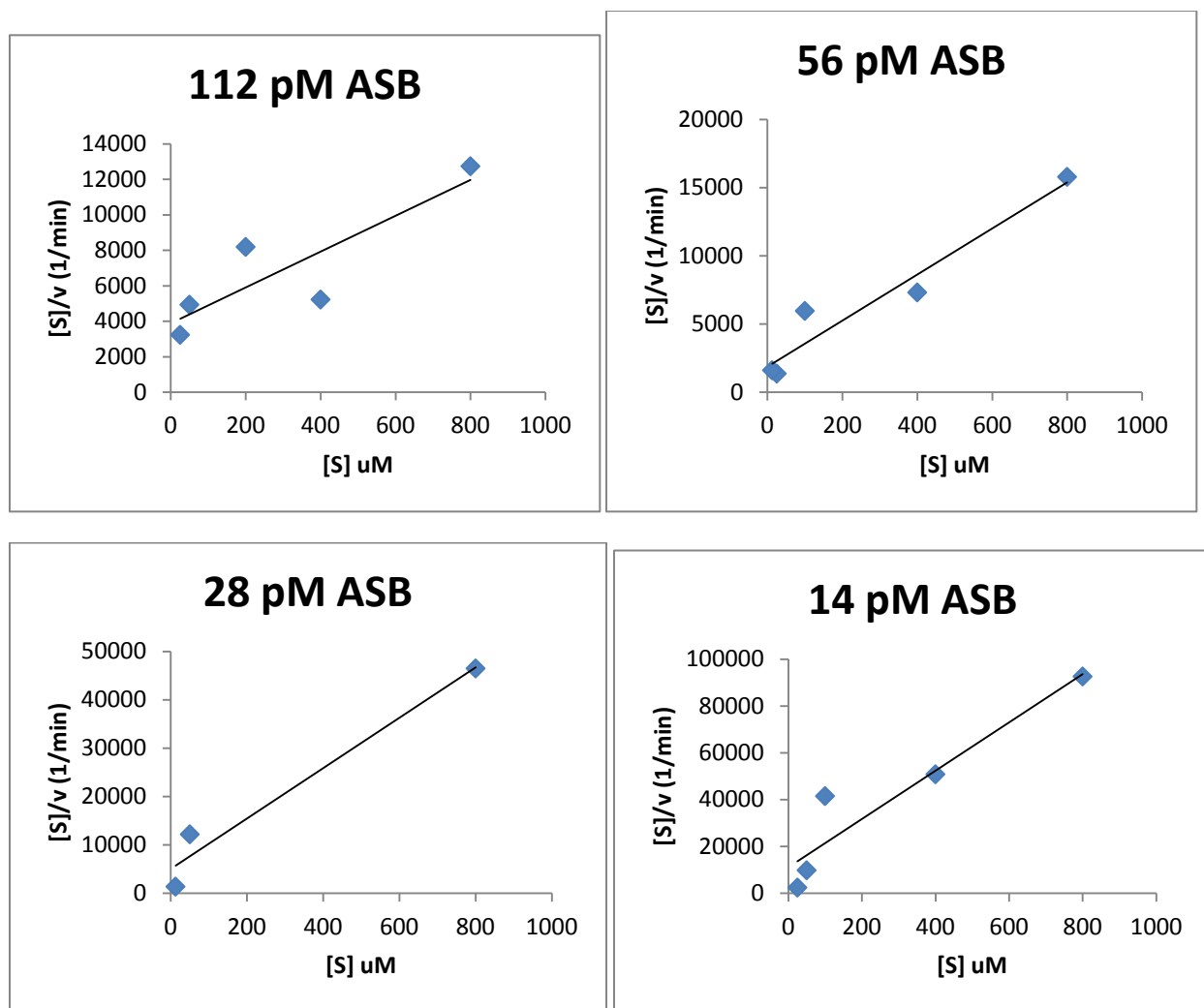


**Figure 4.2.5 Hanes-Woolf plots for 112pM through 14pM ASB** Linear correlation coefficients for the graphs are as follows: 112 pM, 0.864; 56pM, 0.968; 28pM, 0.982; 14pM, 0.943.

As shown in Table 4.2.2, a plateau in the calculated  $k_{cat}$  values was reached between rhASB concentrations of 900pM and 14pM. Table 4.2.3 shows the calculated  $k_{cat}$  and  $K_m$  values for this range, as well as their averages and standard deviations

**Table 4.2.3 Average and Standard deviation of  $K_m$  and  $k_{cat}$  values (900pM – 14pM)**

Concentration of ASB	$K_m$ (uM)	Standard deviation	$k_{cat}$ (1 /min)	Standard deviation
900 pM	190.2		668.6	
450pM	202.2		1012.4	
112 pM	390.9		820.9	
56 pM	112.2		1053.6	
28 pM	96.9		686.1	
14 pM	107.2		692.2	
	<b>183.3</b>	<b>111.2</b>	<b>822.3</b>	<b>172.5</b>

While the coefficients of variation (CV) for the  $K_m$  (61%) and  $k_{cat}$  (21%) are relatively high, this may be related to the noise in the chromatography assay. Taking this noise into account, the desulfation of GalNAc-4S by rhASB under these conditions appears to follow the Michaelis-Menten kinetics, an indication that the problems of both substrate limitation and end-product inhibition have been minimized.

#### **4.3 Attempts to Demonstrate an Intracellular ASB Complex**

BJ (healthy) fibroblasts were grown, lysed, and the lysate applied to a Size Exclusion Chromatography (SEC) column. The purified rhASB standard under the same SEC separation conditions eluted from the column at around 22 minutes, corresponding to its expected elution position based on the molecular weight standards (data not shown). The SEC chromatogram (not shown) of the lysate was featureless, barely emerging from the baseline (the protein content of the lysate is low; the UV detection is not expected to be sensitive enough to detect individual proteins). Fractions were collected every minute and tested for ASB activity using a 4-MUS rhASB activity assay. Four fractions were determined to show detectable ASB enzymatic activity: fractions at 15, 23, 24, and 25 minutes. While fractions 23-25 likely correspond to monomeric ASB, not in a complex with other proteins, fraction 15 eluted at a molecular weight of approximately 250 kDa, indicating that the ASB of the BJ cells was associated with other proteins in this analysis. This is consistent with the hypothesis of a possible protein complex involved in the digestion of GAGs within the lysosome.

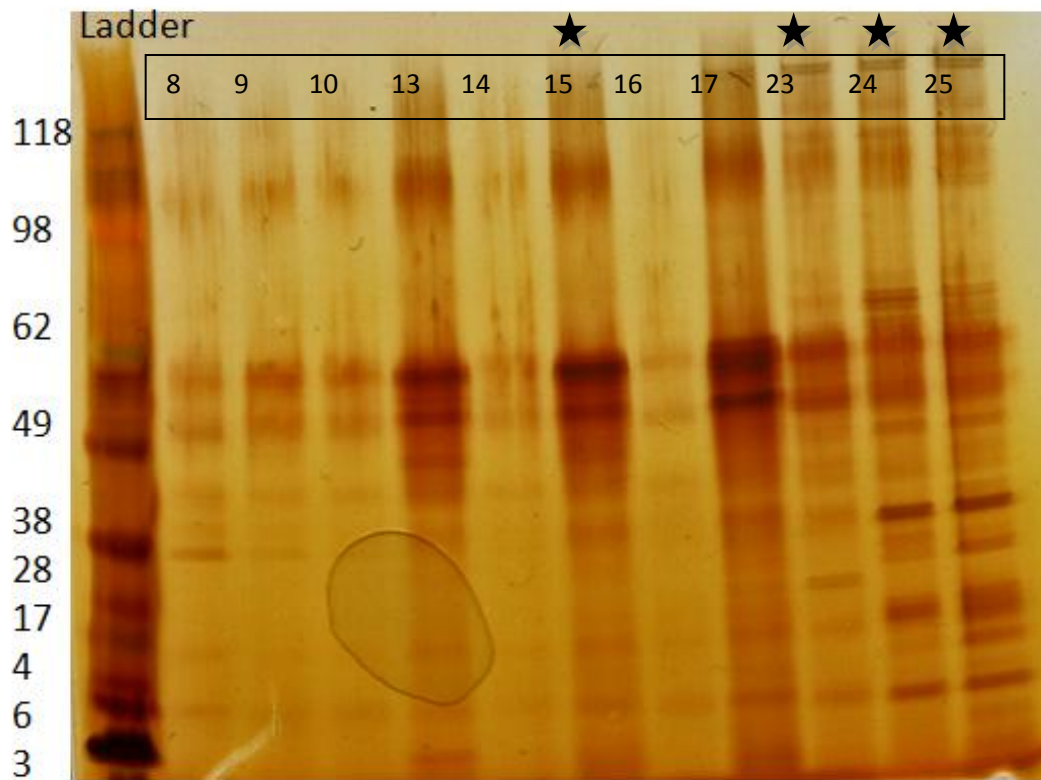


**Figure 4.3.1 Silver Stain of BJ Fibroblasts** Silver Stain of SDS-PAGE gel of fractions 8-10, 13-17, and 23-25 from BJ lysate SEC injection. Lysate of BJ cells was injected onto an SEC column and fractions were collected from 8-26 minutes. Samples with ASB activity and their flanking fractions were run on an SDS-PAGE gel, then silver stained. Invitrogen SeeBlue Plus2 was used as the molecular weight marker. Stars denote fractions that showed ASB activity

The same experiment was then attempted with GM00519 cells supplemented with rhASB to culture medium for five days. The expectation was to observe a similar activity profile to the BJ fibroblast, indicating the formation of a complex with the supplemented rhASB. This would also eliminate the possibility that the ASB activity detected in the high molecular weight region in the earlier experiment is a complex forming during the production of ASB in the healthy cell (as opposed to the hypothesized complex forming to degrade the polysaccharides in the lysosome), as the GM00519 cells would not form this complex. Unfortunately, the experiment with the GM00519 cells supplemented with rhASB was not conclusive, as all fractions within the SEC chromatogram were positive for ASB activity.

## 5. Conclusions

Different methods to observe the enzyme kinetics of the hydrolytic activity of rhASB were utilized, giving insight into the possible mechanism of ASB within the lysosome. Previous studies found a very low turnover rate for a direct assay of a trisaccharide (7 /min), but through a cell-cultured based bioassay of the hydrolytic activity of rhASB, a turnover rate closer to 500/min was found for a the natural polysaccharide chain substrate. Together with the high turnover rate calculated from a direct hydrolysis assay with a monosaccharide substrate (850/min), this supports the hypothesis that ASB works in a different mechanism within the lysosome. This supports the hypothesis that ASB works within a complex within the lysosome to degrade the polysaccharides inside. Even if ASB is the rate-limiting step of the complex, within the complex, the substrate can move from one active site to the next, speeding up the turnover rate and supporting the difference in rate seen between the direct assay for the trisaccharide and the rate seen in the polysaccharide bioassay.

While attempts to demonstrate and isolate this complex were overall inconclusive, there is still strong evidence that this complex is present within the lysosome.

## 6. REFERENCES

- E. Pungor C. Hague, G. Chen** Development of a functional bioassay for arylsulfatase B using the natural substrates of the enzyme [Journal] // Analytical Biochemistry 395. - 2009. - pp. 144-150.
- E. Pungor C. Hague, G. Chen** Development of an Efficacy Indicating Bioassay for rhASB. - January 2009.
- E.F. Neufeld J. Muenzner** The Mucopolysaccharidoses [Book Section] // The Metabolic and Molecular Bases of Inherited Disease / book auth. C.R Scriver A.L. Beudet, W.S. Sly, D. Valle. - New York : McGraw-Hill, 1995. - Vol. 7th ed.
- Iozzo R.V.** Matrix proteoglycans: molecular properties, protein interactions, and role in physiological processes [Journal] // Physiol. Rev. 71. - 1998. - pp. 481-539.
- M. Fuller P.J. Meikle, J. Hopwood** Glycosaminoglycan degradation fragments in mucopolysaccharidosis I [Journal]. - [s.l.] : Glycobiology, 2004. - 443-450 : Vol. 14.
- W. Chen M. Niepel, P. Sorger** Classic and Contemporary Approaches to Modeling Biochemical Reactions [Journal]. - [s.l.] : Genes & Development, 2010. - 17 : Vol. 24.
- W. Hoppe U. Rauch, H. kresse** Degradation of endocytosed dermatan sulfate proteoglycan in human fibroblasts [Journal] // J. Biol. Chem 263. - 1988. - pp. 5926-5932.
- W-D Jin C.E. Jackson, R.J. Desnick, E.H. Schuchman** Mucopolysaccharidosis Type VI: Identification of Three Mutations in the Arylsulfatase B Gene of Patients with the Sever and Mild Phenotypes Provides Molecular Evidence for Genetic Heterogeneity [Journal]. - [s.l.] : Am. J. Hum. Genet, 1992. - pp.795-800 : Vol. 50.



## **Acknowledgements**

Erno Pungor  
Shilpa Shroff  
Chuck Hague  
Ginger Chen  
Crystal Conlan  
Jeff Lemontt

Mary Mead  
Robert Cunico

Dominican University of California Faculty and Staff  
Especially  
Kiowa Bower  
Randall Hall